Optical and Quantum Electronics (2023) 55:948
https://doi.org/10.1007/s11082-023-05203-y

Chitosan/polyaniline/graphene oxide-ferrocene thin film and highly-sensitive surface plasmon sensor for glucose detection

Hassan Nasiri[1] · Hamed Baghban[1] · Reza Teimuri-Mofrad[2] · Ahad Mokhtarzadeh[3]

Received: 13 April 2023 / Accepted: 16 July 2023 / Published online: 19 August 2023

Abstract
This work aims to develop a surface plasmon resonance (SPR) sensor based on Chitosan/Polyaniline/Graphene oxide-Ferrocene (CS/PANI/GOFc) composite thin film for glucose detection. The optimum formulation of the composite has been calculated from experimental refractive index data and using the effective medium theory (EMT). Then, the optimum composite, CS 25%/PANI 25%/GOFc 50%, has been prepared and evaluated in the design of the glucose sensor via modification of the SPR gold chip. Results demonstrate that the linear response of the SPR sensor is in the range of 0.5–100 μM of glucose with a sensitivity of 0.0202° μM^{-1}. The Langmuir and Sips models have been used to analyze the binding affinity, which represents a higher affinity constant for the composite film compared to the bare gold chip.

Keywords Surface plasmon resonance · chitosan · Polyaniline · Graphene oxide · Glucose

1 Introduction

Diabetes as a chronic disease involves the deficiency of insulin production and the inability of cells to respond to insulin; hence, the human body can no longer regulate blood sugar appropriately (Dabelea et al. 2014). Over 500 million cases of diabetes are estimated in 2030, according to the world health organization if they wouldn't be diagnosed

✉ Hassan Nasiri
h.nasiri@tabrizu.ac.ir

✉ Hamed Baghban
h-baghban@tabrizu.ac.ir

Reza Teimuri-Mofrad
Teymori@tabrizu.ac.ir

Ahad Mokhtarzadeh
Mokhtarzadeh@tbzmed.ac.ir

[1] Department of Electrical and Computer Engineering, University of Tabriz, Tabriz, Iran

[2] Department of Organic and Biochemistry, Faculty of Chemistry, University of Tabriz, Tabriz, Iran

[3] Immunology Research Center, Tabriz University of Medical Sciences, Tabriz, Iran

timely (Shaw et al. 2010). So, monitoring blood glucose levels is crucial for human health to prevent hypoglycemia. Currently, diabetes is mainly diagnosed through point-of-care blood glucose tests, an invasive procedure requiring trained personnel. Hence, various sensors containing nanomaterials have been described to quantify glucose levels with improved sensitivities (Xue et al. 2022).

Among the plethora of proposed techniques, surface plasmon resonance (SPR)-based sensors are considered sensitive optical platforms for surface analysis and evaluation of chemical and biological species (Prabowo et al. 2018). Notwithstanding its high sensitivity, SPR sensors have limitations in detecting trace concentrations of glucose, as they measure the refractive index changes on the surface of a gold film (Gumilar et al. 2022). It is assumed that utilizing a coating thin film on a gold chip would increase the refractive index as well as the sensitivity in measuring target analytes (Philip and Kumar 2022). In this regard, nanocomposites provide an attractive approach for modulation of the refractive index and hence, improve the sensitivity of SPR sensors (Li et al. 2022; Wang and Huang 2022), while the main limitation is the determination of optimal nanocomposite formulation.

Polyaniline (PANI), graphene oxide (GO), and Chitosan have attracted significant attention in recent studies of nanocomposite-based sensors due to their unique chemical or electrical characteristics. PANI, as an organic polymer, benefits from excellent stability and high electrical conductivity as a function of Redox states and proton doping. As it responds to different molecular species, it has been successfully used in pH monitoring, energy storage applications, and gas sensing (Beygisangchin et al. 2021). Meanwhile, GO has also been widely used in various biosensor applications thanks to features similar to graphene, accompanied with oxygen-based functional groups on its structure (Perrozzi et al. 2014). Benefiting from both hydrophobic carbon rings and hydrophilic oxygen functionalities such as hydroxyl, epoxy, carboxyl, and carbonyl groups, these features provide interesting characteristics to graphene sheets (Erickson et al. 2010). Moreover, oxygen functional groups behave as anchoring sites to attach to nanoparticles for sensitivity enhancement in biosensors (Yin et al. 2015) and their good dispersion in aquatic media (Lee et al. 2016). These functional groups also offer active sites for immobilizing bio-receptors (Li et al. 2016). For efficient immobilization of sensing components, it is necessary to use appropriate binders such as biocompatible polymers. For this purpose, Chitosan displays high water permeability, film-forming ability, biodegradability, and good adhesion on sensor substrates, which offer a variety of applications in biomedical devices and analytical applications (Rassaei et al. 2008). Several studies have been reported on the application of Chitosan films in the fabrication of SPR sensors (Kamaruddin et al. 2016; Sadrolhosseini et al. 2019; Azeman et al. 2022). To enhance the sensitivity via composite structures, achieving optimum structure and formulation is a tedious and complex procedure by traditional trial and error methods; hence, simulation of multi-layered SPR sensors has been offered as an approach to find optimal criteria via refractive index analysis. Recent studies involve theoretical modeling and evaluation of a multi-layer gold–MoS_2–hBN–graphene for glucose detection based on Fresnel multilayer reflection theory (Mudgal et al. 2020) and mathematical modeling of a graphene-MoS_2 hybrid structure accompanied by TiO_2-SiO_2 nanofilm for formalin detection (Moznuzzaman et al. 2020). The superiority of doped polyaniline compared to thin-film gold/silver in selective sensing of acetone has been proposed in another theoretical study (Usman et al. 2018). Simulation and experimental evaluations of a ZnO/polypyrrole interface for ammonia sensing have been reported in which the thickness of ZnO and PPy have been optimized using a theoretical approach. (Gahlot

et al. 2022), However, there is no report on optimizing composite layers for glucose SPR sensors in the literature; so, that would be interesting to elaborate such structures both theoretically and experimentally.

In this study, for the first time, we have employed the effective medium theory (EMT) to find an optimal composite structure consisting of Chitosan/PANI/GOFc for glucose detection using an SPR platform. Then, the sensor response, sensitivity, and linear operation range are evaluated and compared with a bare gold chip. The experimental results demonstrate the successful utilization of simulation studies in developing the composite layers for modulation of the refractive index for improving the desired features of the SPR sensor for glucose detection.

2 Experimental and theoretical studies

2.1 Reagents and materials

Chitosan and glucose were obtained from Sigma Aldrich (St. Louis, MO, USA). Double distilled and deionized water was used during experiments. The synthesis and characterization of GO, PANI, and GO- Fc nanohybrid nanocomposite were carried out as reported elsewhere (Payami et al. 2020).

2.2 Preparation of glucose solution

Glucose with a concentration of 500 μM was prepared as stock solution and then, the dilution formula, $M_1V_1 = M_2V_2$, was used for serial dilution with deionized water for subsequent analysis.

2.3 Preparation of PBS

A 1 M PBS solution was prepared from K_2HPO_4 and KH_2PO_4 and then 61.5 mL of K_2HPO_4 solution and 38.5 mL of KH_2PO_4 solution were mixed to prepare a solution with pH 7.0.

2.4 Preparation of CS/PANI/GOFc composite thin film combined with SPR

A 25 mg of Chitosan was dissolved in 1 mL of 0.2% Acetic acid in a microtube. In another microtube, 25 mg PANI and 50 mg GOFc were dispersed in 1 mL of deionized water. Finally, the two mixtures were mixed and dispersed for 10 min. Individual solution for each material was also prepared in the same way. Then, approximately 100 μL of each material solution and a composite of them was pipetted on a 50 nm gold-coated glass slip ($10 \times 20 \times 0.1$ mm) followed by spin coating at a speed of 3000 rpm for 30 s. Afterward, the gold/Chitosan/PANI/GOFc thin film was evaporated on the prism surface. It was then placed on an optical stage driven by a stepper motor to carry out the SPR measurements. Finally, 1 mL of Phosphate buffer solution (PBS, PH = 7) as the reference signal was injected into the o-ring and glucose solution with different concentrations ranging from 0.5–100 μM was injected and the SPR spectra were obtained.

2.5 Measuring SPR angles for each component

The SPR angles for each component of nanocomposite (PANI, GOFc, CS) were obtained separately via the SPR device (MP-SPR Navi™ 210A VASA). For this purpose, 50 mg of PANI or GO was dispersed in 1 mL N-Methyl-2-pyrrolidone (NMP), and for CS 5 mg of it was dispersed in a solution containing 0.9 mL NMP and 0.1 mL acetic acid. Then, each mixture was coated separately on the chip surface at 3000 rpm. The reflectance values versus the incident angle were attained for each component experimentally to determine each component's θs (SPR angle).

2.6 Simulation studies

For theoretical studies, the obtained θs via the SPR instrument were used for the calculation of corresponding refractive indices using the following relations (Nguyen and Voronine 2020):

$$k_x = \frac{\omega}{c}\sqrt{\varepsilon_{\text{prism}}} * \sin(\theta) \tag{1}$$

$$\frac{\omega}{c}\sqrt{\varepsilon_{\text{prism}}} * \sin(\theta) = \frac{\omega}{c} * \sqrt{\frac{\varepsilon_1\varepsilon_2\left(\varepsilon_2\mu_1 - \varepsilon_1\mu_2\right)}{\left(\varepsilon_2 - \varepsilon_1\right)\left(\varepsilon_2 + \varepsilon_1\right)}} \tag{2}$$

$$\theta = \arcsin\left(\sqrt{\frac{\varepsilon_2\left(\varepsilon_2\mu_1 - \varepsilon_1\mu_2\right)}{\left(\varepsilon_2 - \varepsilon_1\right)\left(\varepsilon_2 + \varepsilon_1\right)\varepsilon_{\text{prism}}}}\right) \tag{3}$$

where ε_1 and $\varepsilon_{\text{prism}}$ are permittivity values corresponding to the gold and prism, the angle θ is also obtained from the experiments. ε_2 is also related to the component/composite, which is unknown and is calculated from Eq. (3). The reflectance as a function of the angle for each component was calculated using the finite-difference time-domain (FDTD) method, and the simulated results were compared with experimental data.

Then, using the EMT approach (Markel 2016), the effect of each material on the final refractive index of the composite was calculated as:

$$\frac{\varepsilon_R - \varepsilon_h}{\varepsilon_R + 2\varepsilon_h} = f_p\frac{\varepsilon_p - \varepsilon_h}{\varepsilon_p + 2\varepsilon_h} \tag{4}$$

where f_{p} represents the volume percentage of the component, ε_{h} depicts the permittivity value for the host, and ε_{R} and ε_{p} depict the permittivity values for the other two components.

The refractive index values were obtained for various ratios of constituents to find the optimum composition in the nanocomposite, and then, the plasmonic structure was simulated using the FDTD method. Finally, the optimal structure of the nanocomposite was obtained and synthesized experimentally for the SPR sensor development.

2.7 Performance parameters of SPR sensor

The sensitivity (S), full-width half maximum (FWHM), quality factor (QF), and signal-to-noise ratio (SNR) were used as parameters for the evaluation of sensor performance. The high values for S, QF, and DA accompanied by a low value of FWHM are suitable for a desired sensor (Mohanty et al. 2016). Sensitivity is defined as the ratio of the deviation in the SPR angle ($\Delta\theta_{res}$) and the deviation in the sensing medium's RI (Δn). It is mathematically expressed as:

$$S = \Delta\theta_{res}/\Delta n \text{ (in degree/RIU)} \tag{5}$$

The full-width half maxima (FWHM) gives information about the width and sharpness of the reflectance curve and is mathematically expressed as:

$$FWHM = \theta_2 - \theta_1 \text{(in degree)} \tag{6}$$

Also, the quality factor provides information about the resolution of the proposed SPR sensor. It is mathematically expressed with the relation:

$$QF = S/FWHM \left(\text{in } RIU^{-1}\right) \tag{7}$$

Finally, the signal-to-noise ratio (SNR) is the inverse of FWHM. This factor is determined using the SPR curve and mathematically expressed as:

$$SNR = 1/FWHM \left(\text{in degree}^{-1}\right) \tag{8}$$

The linear response range is another important factor that shows the linearity of the sensor in a range of target concentration. All of these parameters have been calculated for developed sensors and compared with previous works.

3 Results and discussion

3.1 Setup consideration of the proposed SPR sensor

The proposed structure of the glucose SPR sensor has been illustrated in Fig. 1, which consists of three layers. The thin gold layer is modified as the main component with optimum CS/PANI/GOFc composite thin film. As the basis of SPR, glucose detection is according to the interaction of p-polarized light with surface plasmons of the thin gold layer, followed by excitation in the Kretschmann arrangement. At the interface of prism-gold, an evanescent field is generated that penetrates the medium with the lower refractive index (at a depth of ~ 150 nm) (Daniyal et al. 2018) and serves as the sensing component because of its high sensitivity to changes in the refractive index. The refractive index changes by the glucose concentration, which influences the coupling of the evanescent wave to the surface plasmons and results in the shift of the SPR reflectance curve (Omar et al. 2019).

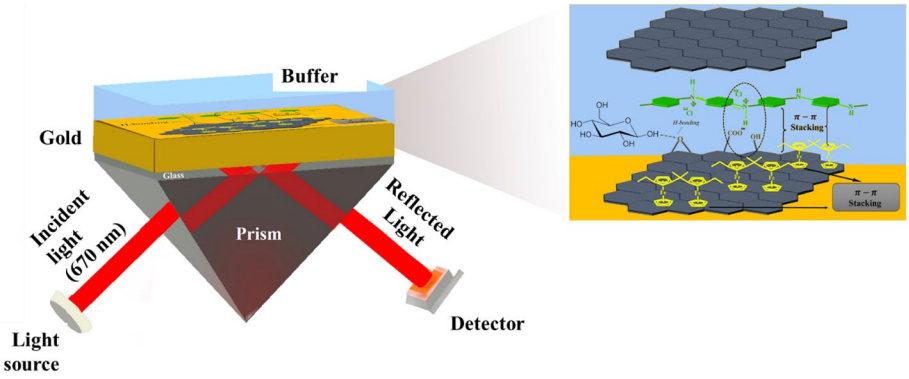

Fig. 1 Schematic of the SPR setup for glucose detection

3.2 Optimization of CS/PANI/GOFc composite layer

Higher frequencies could yield improved optical nonlinearity, and in contrast, improved sensitivity can be achieved with minimum Kerr effect at low frequencies (Maurya et al. 2015). Therefore, the refractive index (RI) for each material was measured at the operating wavelength of 670 nm. In this configuration, the most used component is a prism (BK7 glass) with a refractive index of 1.513 + j3.432e-9. The second region is the gold layer with a complex refractive index of 0.111 + j3.999 and a thickness of 50 nm. The next part, as an adherence layer, is the composite layer of CS/PANI/GO.

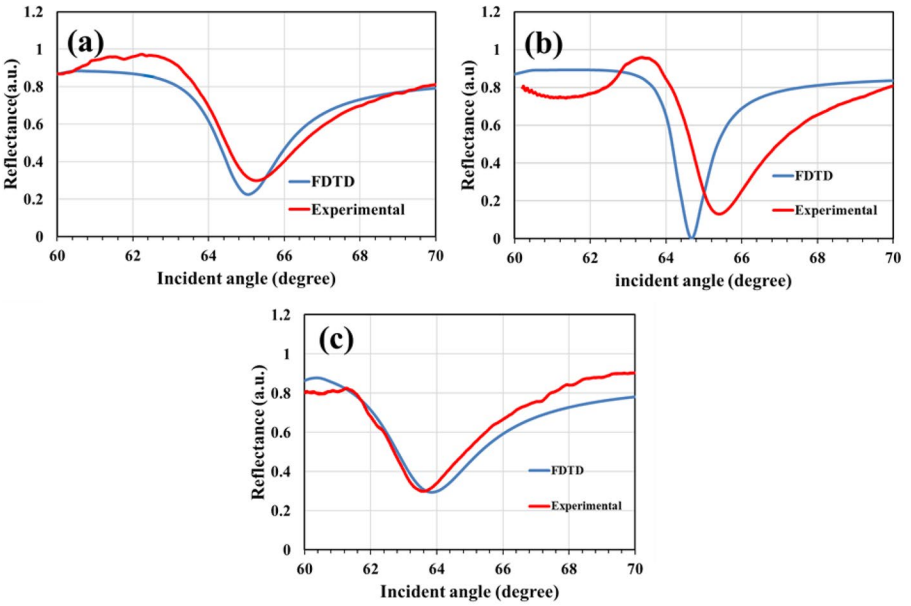

Fig. 2 The FDTD simulation and experimental SPR graphs for gold chip modified by **a** GO, **b** Chitosan, and **c** PANI

For the calculation of the RI, first, the permittivity and RI values for each component of the composite were calculated from the experimental SPR graph, as shown in Fig. 2. The RI values for CS, PANI, and GOFc were obtained using Eq. (3) as 1.627 + j0.131, 1.608 + j0.158, and 1.615 + j0.156, respectively. In addition, as seen in Fig. 2a, a good agreement was obtained between the experimental data and simulation results for GO and PANI using the FDTD method. In the case of Chitosan, a shift to upper angles is observed for experimental data compared to simulation results (Fig. 2b).

On the other hand, as seen in Fig. 3a, when the GOFc serves as host, the RI reduces and θ_{spr} shifts to lower values by increasing the percentage of PANI. Considering the value of the FWHM along with the shift in angle, the optimum percentages of PANI and CS are 25 and 25%, respectively. While for PANI as a host, the RI reduces in intensity accompanied by a shift to larger angles by enhancing the percentage of GOFc and the optimal ratios for GOFc and CS are 25% and 25%, respectively. Comparing the FWHM and shift in angle, the optimum composition for nanocomposite was considered as 50% GOFc and 25% of each PANI and CS (optimal GOFc/PANI/Cs). After that, using the EMT approach, a refractive index of 1.617 + j0.141 was obtained before adsorptions of glucose, and the RI was varied according to the target concentration. Finally, the FDTD simulation and experimental SPR graphs for gold/25% CS/25% PANI/50% GOFc, and experimental SPR graphs for gold chip and gold/25% CS/25% PANI/50% GOFc are given in Fig. 4. As seen, the simulation result approximately matches with experimental SPR graph for the nanocomposite, while the experimental results show that by immobilization of nanocomposite on the surface of the gold chip, the incident angle was increased in charge of a bit reduction in reflectance intensity.

After experimental evaluation, to check the integrity of the optimized nanocomposite film, the surface morphology on the gold chip was examined via the SEM imaging and the result is represented in Fig. 5 at different magnifications. The fragmented sheets of

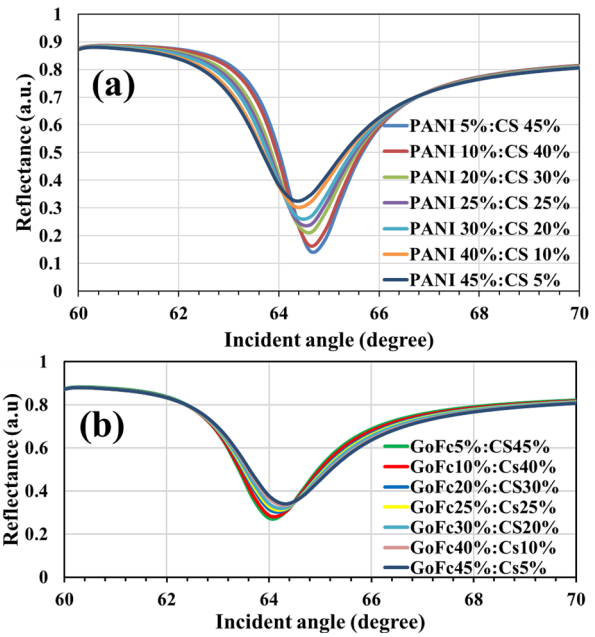

Fig. 3 Optimization of composite layer formulation for SPR sensing in the aqueous phase **a** GOFc as a host matrix (50%) and with varying compositions of PANI and chitosan and **b** PANI as a host matrix (50%) and with varying compositions of GoFc and chitosan from 5 to 45%

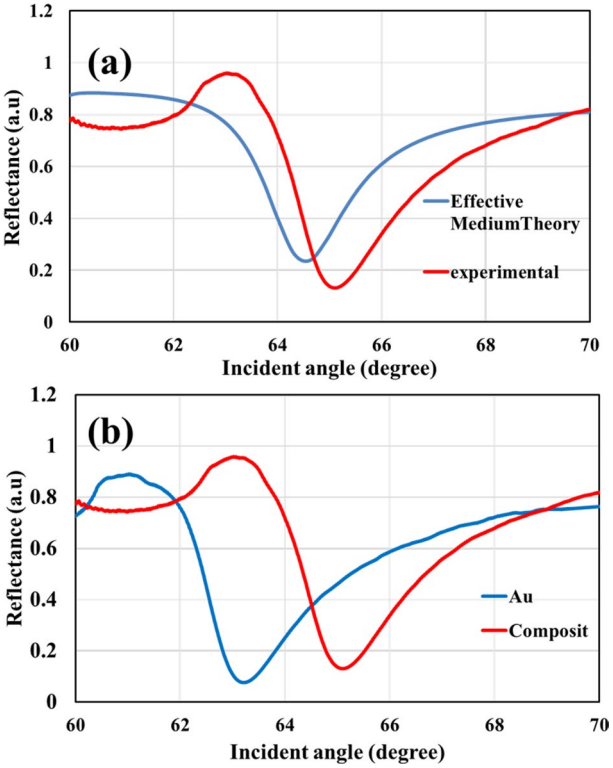

Fig. 4 Comparison of (a) the FDTD simulation and experimental SPR graphs for **a** optimal composite/gold chip, and **b** experimental SPR graphs for bare gold chip and optimal composite/gold chip

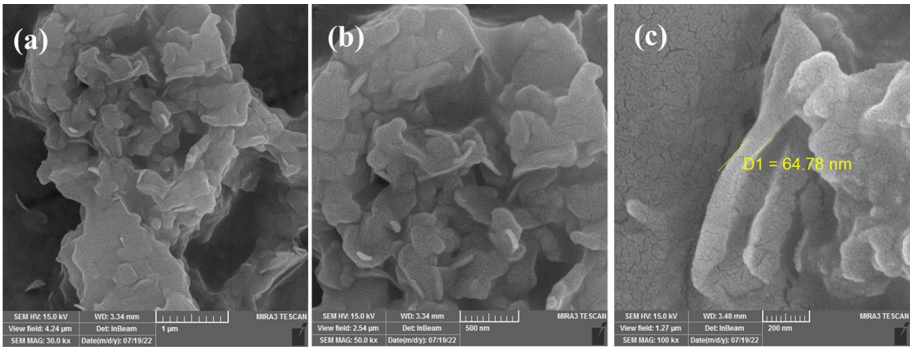

Fig. 5 SEM images of CS/PANI/GOFc thin film on the gold chip at different magnifications of **a** 1 µm, **b** 500 nm, **c** 200 nm

GOFc are attached to the chip surface with enlarged diameters of around 67 nm, which could ascribe to the immobilization of PANI and CS and their efficient integration within the composite film.

3.3 Evanescent fields and SPR reflectance curves for gold chip and gold/CS/PANI/GOFc thin film

Surface plasmon resonance (SPR) sensors use an electromagnetic field called the evanescent field, which is localized at the boundary between a metal layer and a dielectric material like a liquid or glass. The evanescent field doesn't travel far from the metal surface, and it diminishes exponentially as it penetrates only a few hundred nanometers into the dielectric material. It is sensitive to changes in the refractive index of the dielectric material, which enables it to detect analytes on the sensor surface.

In SPR sensors, the evanescent field helps to examine the characteristics of a thin layer of analyte molecules that attach to the metal surface. As analyte molecules bind to the surface, alter the refractive index of the layer, leading to a change in the angle of the reflected light. This change in angle provides information on the amount of analyte attached to the surface and the kinetics of the binding interaction (Maier 2007).

The FDTD Simulations of evanescent fields for bare gold chip and gold/CS/PANI/GOFc thin film are given in Fig. 6. As seen, an improvement has been attained successfully in penetration of the evanescent field into the composite layer from 100 nm for bare gold to 300 nm for composite, which is due to the efficient interaction of the wave with the CS/PANI/GOFc dielectric layer. Such a media can provide an efficient sensitive layer for monitoring the interaction of target glucose molecules with the composite layer.

The SPR reflectance curve of the thin gold layer contacted with PBS for 10 min is given in Fig. 7a. The obtained resonance angle was 63.211°. Then, glucose solutions with different concentrations ranging from 0.5 to 500.0 µM were added and the detection was performed. From the inset of Fig. 7, the resonance angles for all glucose concentrations and PBS showed negligible differences as there is no or negligible change in the refractive index of the glucose solutions. Therefore, the gold thin film-based SPR sensor could not detect and differentiate in measuring minor changes in the refractive index of PBS and low concentration of glucose solution (Zainudin et al. 2018).

The surface of the gold film was then modified with the optimal CS/PANI/GOFc composite layer to enhance the SPR sensor's sensitivity. The curves for the SPR reflectance of the gold/CS/PANI/GOFc thin film contacted with PBS are illustrated in Fig. 7b, which represents a resonance angle of 65.110°, a value slightly higher than the previous resonance angle for the thin gold layer. A 1.899° rise in the resonance angle is owing to the variation in the refractive index of the chip surface resulting from the immobilization of the CS/PANI/GOFc layer that disturbs the resonance state (Fen et al. 2015).

Glucose solutions with different concentrations ranging from 0.5 to 500.0 µM were then injected into the device containing the gold chip modified by optimal CS/PANI/GOFc surface. As shown in Fig. 7b, an increase in the resonance angle is obtained which shifts to larger resonance angles with increasing the solution concentration. Table 1 presents the resonance angle shift at different concentrations of the glucose solution where the increasing shift in the resonance angle with the refractive index demonstrates the effective binding and interaction of glucose molecules to the surface of gold/CS/PANI/GOFc thin film (Anas et al. 2020). Such interactions will be evaluated in the following section. It is noteworthy that the gold/CS/PANI/GOFc thin film shows a substantial variation in resonance angle while sensing even the glucose concentrations as low as 0.5 µM.

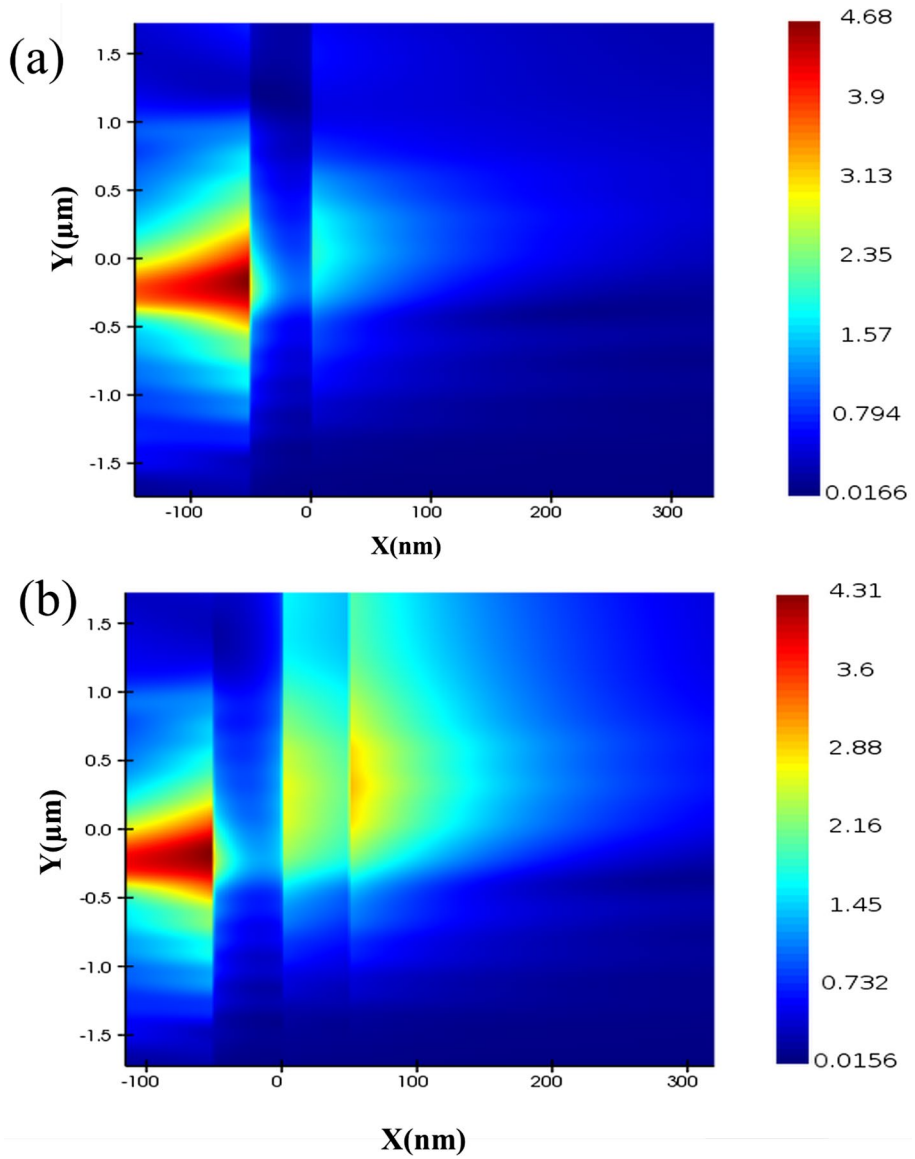

Fig. 6 The FDTD simulation of evanescent fields for **a** bare gold chip and **b** gold/CS/PANI/GOFc chip

3.4 Sensitivity evaluation and binding affinity estimation

To measure the sensitivity of the sensor, a linear correlation of SPR response and glucose concentration in solution was established using the linear fit tool in Origin 9 software. Figure 8 depicts the linear fit for the bare gold chip and gold chip modified by optimalCS/ PANI/GOFc thin film. The slope of the line obtained from the linear regression analysis for the former as the sensor sensitivity was 0° μM^{-1}, where there was no

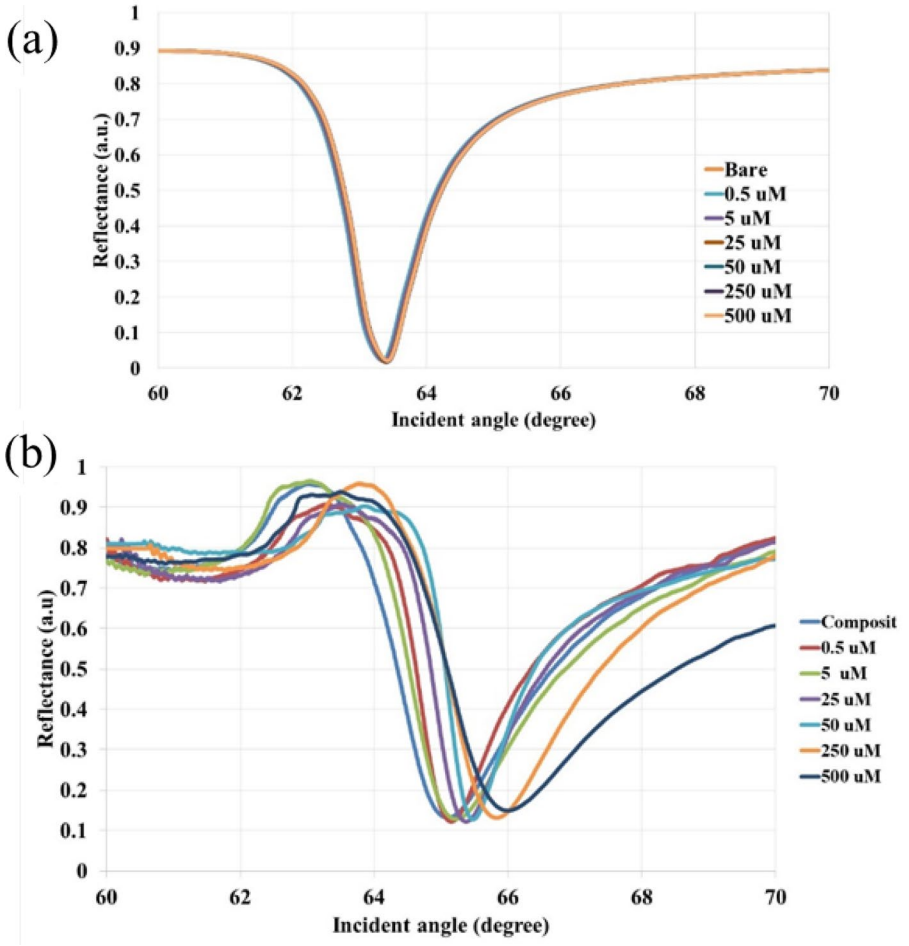

Fig. 7 SPR reflectance curves of **a** bare gold chip, **b** gold chip modified by optimal CS/PANI/GOFc thin film contacted with various concentrations of glucose solution ranged from 0.5–500 μM

Table 1 Properties of the SPR glucose biosensor

Concentration [μM]	Resonance angle (θ)	Shift of resonance angle (Δθ)	Sensitivity	FWHM	FOM	SNR
0	65.11	0		1.2269	–	0.6066
0.5	65.148	0.038	64.40678	1.2444	52.757	0.6029
5	65.222	0.112	172.093	1.4440	119.175	0.69225
25	65.469	0.359	320.779	1.64543	194.954	0.8150
50	65.48	0.37	153.521	1.6584	92.5711	0.8035
250	65.84	0.73	110.084	1.7698	62.153	0.5641
500	66.013	0.903	103.0387	2.04329	50.427	0.4814

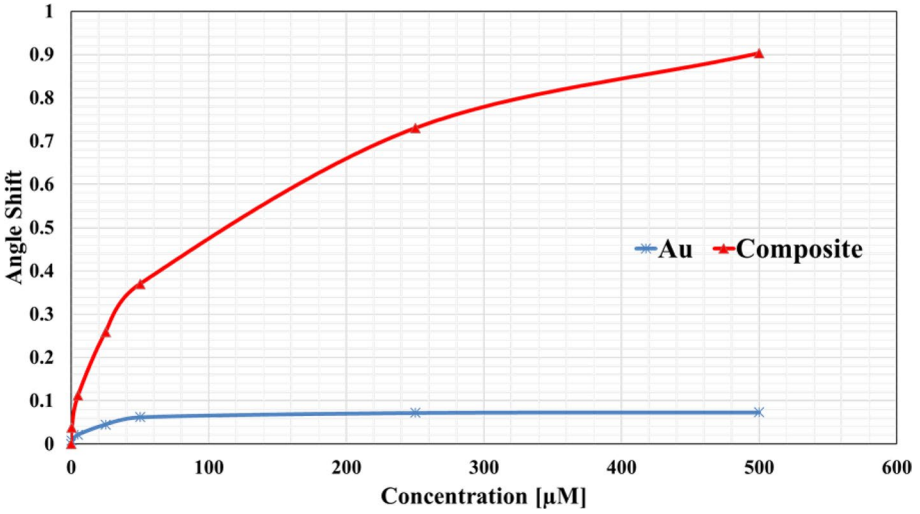

Fig. 8 The shift of resonance angle for gold thin film and gold/25% CS/25% PANI/50% GOFc thin film

Table 2 Comparison of the characteristics of the proposed biosensor with other structures

Active layer	Detection range	Detection limit	QF	Reference
Gold/Silver/SiO_2	3.9–5.6 mM	3.9 mM	56.5	(Omidniaee et al. 2021)
Ag/ZnSe	0.835–560 mM	0.835 mM	66.41	(El-assar et al. 2023)
Gold–MoS_2–hBN–graphene	0.835–560 mM	0.835 mM	16.04	(Mudgal et al. 2020)
Gold/CS/PANI/ GOFc	0.5–100 µM	0.5 µM	194.954	This work

change in the refractive index of the gold chip for all concentrations of the target. In contrast, for linear regression analysis of gold/composite thin film, the slope line was divided into three parts, exposing the sensitivities of 0.0131° μM^{-1} and 0.0011° μM^{-1} for the concentrations of 0.5 to 25 µM and 25–500 µM, respectively. Thus, this SPR sensor can detect glucose down to 0.5 µM and exhibits a sensitivity of 0.0131° μM^{-1}. Lastly, the operation characteristics of the introduced sensor compared with recent glucose detection studies using SPR sensors as presented in Table 2. Results demonstrate that the introduced sensor has a comparable detection limit and sensitivity with improved response range, signifying that the composite layer boosts the performance of the SPR sensor.

To estimate the binding affinities of SPR sensors based on bare gold chip and gold/ CS/ PANI/ GOFc thin film towards glucose molecules, the non-linear fitting according to the Langmuir isotherm model was utilized (Fig. 9a). The Langmuir isotherm model is as follows [53]:

$$\Delta\theta = \frac{\Delta\theta_{\max} C}{\frac{1}{K} + C} \tag{9}$$

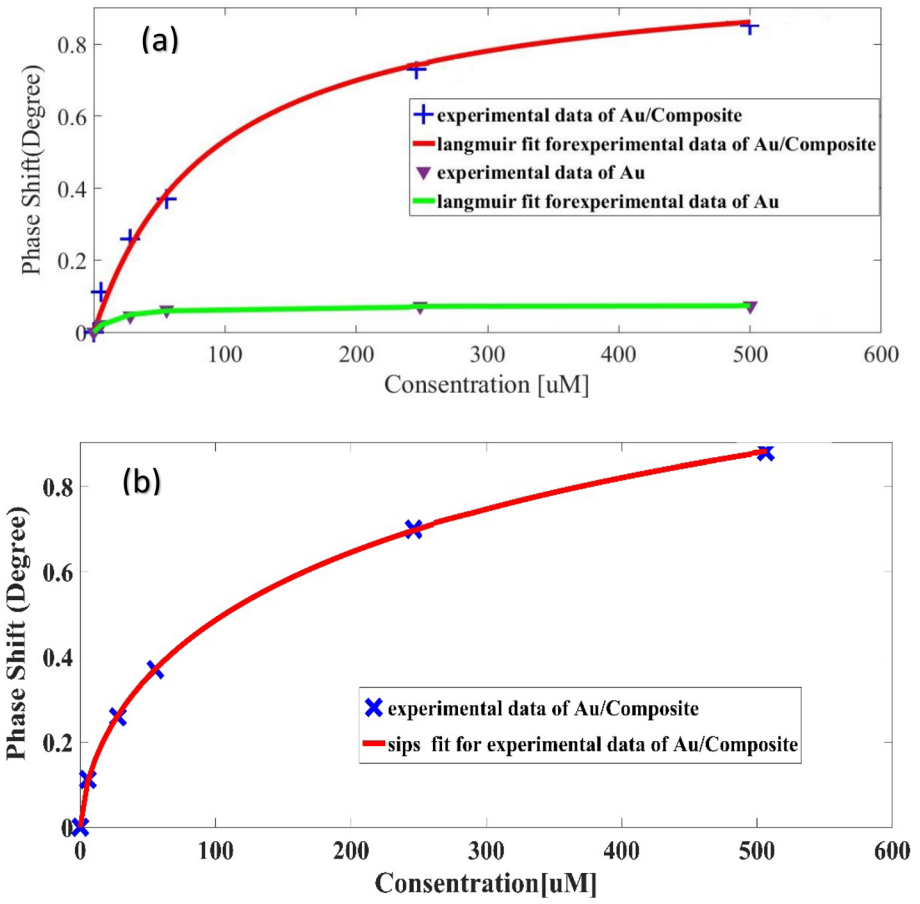

Fig. 9 The estimation of binding affinity according to **a** Langmuir and **b** Sips isotherm models for various concentrations of glucose solution contacted with bare gold chip and gold/CS/ PANI/ GOFc composite

Here, C is glucose concentration, Δθ denotes the shift in resonance angle, and K depicts the binding affinity. The estimated value for the affinity constant of the glucose to gold film is 0.9018 μM^{-1}, while for gold/ CS/ PANI/GOFc thin film is 157.143 μM^{-1}. It is noteworthy to mention that the thin film has a higher affinity constant and hence, stronger interaction with glucose molecules compared with the bare gold chip (Daniyal et al. 2019). To estimate the heterogenous surface of the electrode, the experimental data for gold/25% CS/25% PANI/50% GOFc thin film was also fitted to the Sips isotherm model:

$$\Delta\theta = \frac{\Delta\theta_{\max}(KsC)^n}{1+(KsC)^n} \tag{10}$$

Ks in Eq. (6) denotes the Sips affinity value, C represents the glucose concentration, and n is the heterogeneity constant in the range of 0 to 1 (Saleviter et al. 2019). As seen in Fig. 9b, the data is in close-fitting to the Sips model ($R^2 = 0.9978$) compared to the

Langmuir model ($R^2 = 0.9917$), and an n-value of 0.38 is obtained representing a heterogenous surface phenomenon.

4 Conclusions

In this study, a composite of CS, PANI, and GOFc was first optimized via theoretical studies involving experimental refractive index data and the EMT approach. Simulation results showed better behavior of the composite with constituents of 25% CS/25% PANI/50% GOFc. The SPR sensor with the optimal composite thin film was then prepared and experimentally evaluated for glucose detection. The designed SPR sensor presented enhanced refractive index variations when interacting with glucose solution compared to the unmodified gold chip. More importantly, the introduced SPR sensor has higher sensitivity (0.0202° μM^{-1}) with a detectable glucose concentration of 0.5 μM. Also, the affinity of the sensor to glucose was evaluated using the Sips model which showed a value of 6.39 μM^{-1}. The obtained findings signify that this novel composite thin film based on CS, GOFc, and PANI could be a considerable candidate as a gold chip modifier for glucose sensing.

Acknowledgements We kindly acknowledge the facilities provided by the University of Tabriz and Tabriz University of Medical Sciences.

Author contributions Conceptualization, methodology, writing—original draft preparation, H. N.; validation, supervision, writing—review and editing, funding acquisition, H. B.; formal analysis, writing—review and editing, R.T-M., A. M.; All authors have read and agreed to the published version of the manuscript. All authors read and approved the final manuscript.

Funding This work did not get any funding.

Data availability The data and materials in this paper can be accecced through the journal instrcutions.

Declarations

Conflict of interests There is no competing interests to deaclare.

Ethical approval Not applicable.

References

Anas, N.A.A., Fen, Y.W., Yusof, N.A., Omar, N.A.S., Daniyal, W.M.E.M.M., Ramdzan, N.S.M.: Highly sensitive surface plasmon resonance optical detection of ferric ion using CTAB/hydroxylated graphene quantum dots thin film. J. Appl. Phys. **128**(8), 083105 (2020)

Azeman, N.H., Bakar, M.H.A., Nazri, N.A.A., Mobarak, N.N., Khushaini, M.A.A., Aziz, T.H.T.A., Zain, A.R.M., Bakar, A.A.A.: Carboxymethyl chitosan/graphene oxide/silver nanotriangles nanohybrid as the sensing materials for the enhancement of ammonia localized surface plasmon resonance sensor. Opt. Laser Technol. **148**, 107789 (2022)

Beygisangchin, M., Abdul Rashid, S., Shafie, S., Sadrolhosseini, A.R., Lim, H.N.: Preparations, properties, and applications of polyaniline and polyaniline thin films—a review. Polymers **13**(12), 2003 (2021)

Dabelea, D., Mayer-Davis, E.J., Saydah, S., Imperatore, G., Linder, B., Divers, J., Bell, R., Badaru, A., Talton, J.W., Crume, T.: Prevalence of type 1 and type 2 diabetes among children and adolescents from 2001 to 2009. JAMA **311**(17), 1778–1786 (2014)

Daniyal, W., Saleviter, S., Fen, Y.W.: Development of surface plasmon resonance spectroscopy for metal ion detection. Sens. Mater **30**(9), 2023–2038 (2018)

Daniyal, W.M.E.M.M., Fen, Y.W., Abdullah, J., Sadrolhosseini, A.R., Saleviter, S., Omar, N.A.S.: Label-free optical spectroscopy for characterizing binding properties of highly sensitive nanocrystalline cellulose-graphene oxide based nanocomposite towards nickel ion. Spectrochim. Acta Part A Mol. Biomol. Spectrosc. **212**, 25–31 (2019)

El-assar, M., Taha, T.E., El-Samie, F.E.A., Fayed, H.A., Aly, M.H.: ZnSe-based highly-sensitive SPR biosensor for detection of different cancer cells and urine glucose levels. Opt. Quant. Electron. **55**(1), 76 (2023)

Erickson, K., Erni, R., Lee, Z., Alem, N., Gannett, W., Zettl, A.: Determination of the local chemical structure of graphene oxide and reduced graphene oxide. Adv. Mater. **22**(40), 4467–4472 (2010)

Fen, Y.W., Yunus, W.M.M., Yusof, N.A., Ishak, N.S., Omar, N.A.S., Zainudin, A.A.: Preparation, characterization and optical properties of ionophore doped chitosan biopolymer thin film and its potential application for sensing metal ion. Optik **126**(23), 4688–4692 (2015)

Gahlot, A.P.S., Paliwal, A., Kapoor, A.: Theoretical and Experimental investigation on SPR Gas Sensor Based on ZnO/polypyrrole interface for ammonia sensing applications. Plasmonics **2022**, 1–14 (2022)

Gumilar, G., Henzie, J., Yuliarto, B., Patah, A., Nugraha, N., Iqbal, M., Amin, M.A., Hossain, M.S.A., Yamauchi, Y., Kaneti, Y.V.: Performance enhancement strategies of surface plasmon resonance sensors in direct glucose detection using pristine and modified UiO-66: effects of morphology, immobilization technique, and signal amplification. J. Mater. Chem. a. **10**(12), 6662–6678 (2022)

Kamaruddin, N.H., Bakar, A.A.A., Yaacob, M.H., Mahdi, M.A., Zan, M.S.D., Shaari, S.: Enhancement of chitosan-graphene oxide SPR sensor with a multi-metallic layers of Au–Ag–Au nanostructure for lead (II) ion detection. Appl. Surf. Sci. **361**, 177–184 (2016)

Lee, J., Kim, J., Kim, S., Min, D.-H.: Biosensors based on graphene oxide and its biomedical application. Adv. Drug Deliv. Rev. **105**, 275–287 (2016)

Li, D., Zhang, W., Yu, X., Wang, Z., Su, Z., Wei, G.: When biomolecules meet graphene: from molecular level interactions to material design and applications. Nanoscale **8**(47), 19491–19509 (2016)

Li, L.-J., Wang, X.-Q., Li, J.-W., Jia, Q.-Y., Yang, H.-J., Bo, Y.-Q., Liu, Z.-Q., Zhang, P.-F., Kong, L.-X.: Sensitivity-enhanced fiber-optic surface plasmon resonance sensor utilizing Cu/WS2/PAAG composite film for pH measurement. Optik **260**, 169075 (2022)

Maier, S.A.: Plasmonics: fundamentals and applications. Springer (2007)

Markel, V.A.: Introduction to the Maxwell Garnett approximation: tutorial. JOSA A **33**(7), 1244–1256 (2016)

Maurya, J., Prajapati, Y., Singh, V., Saini, J., Tripathi, R.: Performance of graphene–MoS2 based surface plasmon resonance sensor using Silicon layer. Opt. Quant. Electron. **47**(11), 3599–3611 (2015)

Mohanty, G., Akhtar, J., Sahoo, B.K.: Effect of semiconductor on sensitivity of a graphene-based surface plasmon resonance biosensor. Plasmonics **11**, 189–196 (2016)

Moznuzzaman, M., Islam, M.R., Hossain, M.B., Mehedi, I.M.: Modeling of highly improved SPR sensor for formalin detection. Results Phys. **16**, 102874 (2020)

Mudgal, N., Saharia, A., Agarwal, A., Ali, J., Yupapin, P., Singh, G.: Modeling of highly sensitive surface plasmon resonance (SPR) sensor for urine glucose detection. Opt. Quant. Electron. **52**(6), 1–14 (2020)

Nguyen, D., Voronine, D.: Calculating resonance angle for surface plasmon resonance activation on different metals. Undergrad. J. Math. Model: One + Two **11**(1), 8 (2020)

Omar, N.A.S., Fen, Y.W., Saleviter, S., Daniyal, W.M.E.M.M., Anas, N.A.A., Ramdzan, N.S.M., Roshidi, M.D.A.: Development of a graphene-based surface plasmon resonance optical sensor chip for potential biomedical application. Materials **12**(12), 1928 (2019)

Omidniaee, A., Karimi, S., Farmani, A.: Surface plasmon resonance-based SiO_2 Kretschmann configuration biosensor for the detection of blood glucose. SILICON **2021**, 1–10 (2021)

Payami, E., Ahadzadeh, I., Mohammadi, R., Teimuri-Mofrad, R.: Design and synthesis of novel binuclear ferrocenyl-intercalated graphene oxide and polyaniline nanocomposite for supercapacitor applications. Electrochim. Acta **342**, 136078 (2020)

Perrozzi, F., Prezioso, S., Ottaviano, L.: Graphene oxide: from fundamentals to applications. J. Phys.: Condens. Matter **27**(1), 013002 (2014)

Philip, A., Kumar, A.R.: The performance enhancement of surface plasmon resonance optical sensors using nanomaterials: a review. Coord. Chem. Rev. **458**, 214424 (2022)

Prabowo, B.A., Purwidyantri, A., Liu, K.-C.: Surface plasmon resonance optical sensor: a review on light source technology. Biosensors **8**(3), 80 (2018)

Rassaei, L., Sillanpää, M., Marken, F.: Modified carbon nanoparticle-chitosan film electrodes: physisorption versus chemisorption. Electrochim. Acta **53**(19), 5732–5738 (2008)

Sadrolhosseini, A.R., Rashid, S.A., Jamaludin, N., Noor, A., Isloor, A.M.: Surface plasmon resonance sensor using polypyrrole-chitosan/graphene quantum dots layer for detection of sugar. Mater. Res. Express **6**(7), 075028 (2019)

Saleviter, S., Fen, Y.W., Daniyal, W.M.E.M.M., Abdullah, J., Sadrolhosseini, A.R., Omar, N.A.S.: Design and analysis of surface plasmon resonance optical sensor for determining cobalt ion based on chitosan-graphene oxide decorated quantum dots-modified gold active layer. Opt. Express **27**(22), 32294–32307 (2019)

Shaw, J.E., Sicree, R.A., Zimmet, P.Z.: Global estimates of the prevalence of diabetes for 2010 and 2030. Diabetes Res. Clin. Pract. **87**(1), 4–14 (2010)

Usman, F., J. Dennis and F. Meriaudeau.: Development of a surface plasmon resonance acetone sensor for noninvasive screening and monitoring of diabetes. In IOP Conference Series: Materials Science and Engineering, IOP Publishing. (2018)

Wang, G., Huang, L.: Sensitivity enhancement of a silver based surface plasmon resonance sensor via an optimizing graphene-dielectric composite structure. Appl. Opt. **61**(3), 683–690 (2022)

Xue, Y., Thalmayer, A.S., Zeising, S., Fischer, G., Lübke, M.: Commercial and scientific solutions for blood glucose monitoring—a review. Sensors **22**(2), 425 (2022)

Yin, P.T., Shah, S., Chhowalla, M., Lee, K.-B.: Design, synthesis, and characterization of graphene–nanoparticle hybrid materials for bioapplications. Chem. Rev. **115**(7), 2483–2531 (2015)

Zainudin, A.A., Fen, Y.W., Yusof, N.A., Al-Rekabi, S.H., Mahdi, M.A., Omar, N.A.S.: Incorporation of surface plasmon resonance with novel valinomycin doped chitosan-graphene oxide thin film for sensing potassium ion. Spectrochim. Acta Part A Mol. Biomol. Spectrosc. **191**, 111–115 (2018)